Diffractive SUSY particle production at the LHC

M. Boonekamp*
Service de physique des particules, CEA/Saclay, 91191 Gif-sur-Yvette cedex, France

J. Cammin†
University of Rochester, NY, USA

S. Lavignac‡ and R. Peschanski§
Service de physique théorique, CEA/Saclay, 91191 Gif-sur-Yvette cedex, France¶

C. Royon**
Service de physique des particules, CEA/Saclay, 91191 Gif-sur-Yvette cedex, France, and Fermilab, Batavia, USA

We give detailed predictions for diffractive SUSY Higgs boson and top squark associated productions at the LHC via the exclusive double pomeron exchange mechanism. We study how the SUSY Higgs cross section and the signal-over-background ratio are enhanced as a function of $\tan\beta$ in different regimes. The prospects are particularly promising in the "anti-decoupling" regime, which we study in detail. We also give the prospects for a precise measurement of the top squark mass using the threshold scan of central diffractive associated top squark events at the LHC.

I. INTRODUCTION

The quest for supersymmetry (SUSY) is one of the major goals in high energy particle physics, and is obviously a most exciting one for experiments to be held at the LHC. Discovering SUSY Higgs scalar(s) and opening new SUSY particle thresholds, among which the superpartners of the top quark are good candidates, would be a fantastic achievement. Standard production mechanisms based on QCD are now well explored, at least for the main channels. However, both the general interest of the problem and some specific features of the Higgs and top squark sector of the SUSY models call for investigations allowing to open new promising ways of SUSY production. It is our purpose to investigate in a concrete way the prospects for diffractive production of SUSY Higgs bosons and associated sparticles (stops) in the central region of the detectors.

The subject of the Standard Model Higgs boson production in double diffraction (denoted DPE, for Double Pomeron Exchange) has already drawn considerable interest in recent years [1, 2, 3], [4, 5, 6, 7, 8]. Many approaches have been pursued, considering diffractive scattering, as in the Regge picture [1, 2, 3], as final state soft colour interactions [6], or as fully perturbative exchange of gluon pairs [7]. We extend this study here to the SUSY Higgs and sparticle sector.

One generally considers two types of DPE events for the production of a heavy state, namely "exclusive" DPE [1, 2, 3], where the central heavy object is produced alone, separated from the outgoing hadrons by rapidity gaps :

$$pp \to p + \text{heavy object} + p \ , \tag{1}$$

and "inclusive" DPE [4, 5, 6, 7, 8], where the colliding Pomerons are resolved (very much like ordinary hadrons), dressing the central object with Pomeron "remnants" (X,Y):

$$pp \to p + X + \text{heavy object} + Y + p \ . \tag{2}$$

In general, exclusive production is considered most promising, since one expects a good signal-over-background ratio due to the large gaps with no or low hadronic activity specific of diffractive events and to the good missing mass resolution [9]. Obviously, hard diffractive cross-sections are of higher order than standard hard non-diffractive ones,

---

¶ URA 2306, unité de recherche associée au CNRS.

*Electronic address: boon@hep.saclay.cea.fr
†Electronic address: cammin@fnal.gov
‡Electronic address: lavignac@spht.saclay.cea.fr
§Electronic address: pesch@spht.saclay.cea.fr
**Electronic address: royon@hep.saclay.cea.fr

and this implies lower cross-sections. It is the purpose of the present paper to make some concrete evaluation. We will focus on exclusive production (1) and stick to the original Bialas-Landshoff type of models [1, 2, 4], with their extension to SUSY Higgs and stop production which we will develop in the next sections. It will be easy to use our methods to extend the study to other models. Specifically, a recently developed Monte-Carlo program, `DPEMC` [25], implements the models of [1, 2, 3, 5, 7]. Moreover, most of the plots are in terms of s/b and enhancement factors, that are independent of the models.

It is important to note that although a less appealing search channel, inclusive DPE (2) is important to consider since it constitutes a background to exclusive DPE. Besides, it should not be forgotten that of the above two, only inclusive DPE has actually been observed for high central masses [10].

Due to the limitation in the available total energy for production, it is clear that diffractive production is favoured for the production of SUSY particles in the lower range of their mass in the admissible set of model parameters. Hence, we will focus on this range for the SUSY Higgs sector and for top squarks, respectively. Note that the regions of parameter space that favour the light Higgs boson and the light top squarks are not the same, so a specific study is required separately for Higgs bosons and top squarks. It will be done in turn in two different sections of our paper.

It is well-known that the Higgs boson sector of the Minimal Supersymmetric Standard Model (MSSM) [11] is richer than that of the Standard Model. First, it contains five physical scalar degrees of freedom, instead of a single one: two CP-even neutral Higgs bosons h and H, a pseudoscalar Higgs bosons A and a charged Higgs boson pair $H^{\pm}$. Secondly, the lightest MSSM Higgs boson h may look very different from the SM Higgs boson. In fact, one can define (at least) three noteworthy regimes for the couplings of the neutral MSSM Higgs bosons h, H and A:

(i) the *decoupling* regime, in which h behaves like the SM Higgs boson [12, 13];

(ii) the *intense coupling* regime, in which the couplings of all three neutral Higgs bosons are very different from those of the SM Higgs boson [14];

(iii) the so-called *anti-decoupling* regime [15], in which H behaves like the SM Higgs boson, while h has enhanced (resp. suppressed) couplings to down-type fermions (resp. up-type fermions and gauge bosons) [16].

It is well-known that the SUSY Higgs boson sector contains at least one scalar h with rather low mass (the other, H, being with larger but possibly accessible mass) which gives a particular interest for diffractive production as we will study in detail in this paper. Indeed, the small mass and the sometimes small rate and always experimentally difficult detection in the standard $\gamma\gamma$ channel enhances the interest in alternative production modes and decays such as diffractive production. We will in particular focus on central diffractive production of the lightest MSSM Higgs boson in the anti-decoupling regime (iii) which has not yet been intensively studied in the proposed framework[1].

The interest of SUSY Higgs boson production via exclusive diffractive production parallels a similar analysis for the Standard Model Higgs boson, with some distinctive features which enhance the specific production and branching modes.

The discovery of "sparticles" at the LHC would be the clearest and most exciting signal of new fundamental physics beyond the Standard Model. Among these the scalar superpartners of the top quark are expected to be those with smallest mass among scalars in most MSSM models. Indeed, various supersymmetric scenarios can accommodate a light top squark consistent with the experimental bounds on other sparticle masses and with measurements of observables that could be affected by large supersymmetric contributions, such as the anomalous magnetic moment of the muon or the branching ratio of the flavour violating decay $b \to s\gamma$. Minimal supergravity [18] (mSUGRA) scenarios with a light top squark typically require a low gaugino mass parameter $m_{1/2}$ and a large A-term parameter A_0. The need for a small $m_{1/2}$ is due to the fact that the renormalization group equations for the soft supersymmetry breaking squark masses M_Q^2 and M_R^2 receive a large contribution from gluinos: the larger $m_{1/2}$, the higher the weak-scale values of $M_{Q_3}^2$ and $M_{U_3}^2$. As an example, the Snowmass Point 5 (SPS 5), defined by the following values of the mSUGRA parameters: $m_0 = 150$ GeV, $m_{1/2} = 300$ GeV, $A_0 = -1000$ GeV, $\tan\beta = 5$ and $\mathrm{sign}(\mu) = +$, yields the following top squark and sbottom spectrum [19], as generated by the program SUSYGEN 3.00/27 [20]:

$$m_{\tilde{t}_1} = 210 \text{ GeV} , \qquad m_{\tilde{t}_2} = 632 \text{ GeV} , \qquad m_{\tilde{b}_1} = 561 \text{ GeV} , \qquad m_{\tilde{b}_2} = 654 \text{ GeV} . \tag{3}$$

For comparison, a "typical" mSUGRA scenario with vanishing A_0, the "post-WMAP benchmark scenario" B', defined by $m_0 = 60$ GeV, $m_{1/2} = 250$ GeV, $A_0 = 0$, $\tan\beta = 10$ and $\mathrm{sign}(\mu) = +$, yields [21]:

$$m_{\tilde{t}_1} = 393 \text{ GeV} , \qquad m_{\tilde{t}_2} = 573 \text{ GeV} , \qquad m_{\tilde{b}_1} = 502 \text{ GeV} , \qquad m_{\tilde{b}_2} = 528 \text{ GeV} . \tag{4}$$

---

[1] The intense coupling regime has been studied in Ref. [17], where it is claimed that diffractive Higgs boson production can help distinguishing between h and H.

Light top squarks and bottom squarks [2] can also arise from non-minimal SUGRA models, e.g. from scenarios with an inverted mass hierarchy in the squark sector [22]. Assuming $M^2_{\Phi_3} \ll M^2_{\Phi_{1,2}}$ ($\Phi = Q, U, D$) at the GUT scale and small gaugino masses, one ends up with very low third generation squark masses at the weak scale due to strong 2-loop renormalization group effects proportional to $\alpha_S^2 \mathrm{Tr}(2M_Q^2 + M_U^2 + M_D^2)$ [23]. The first two squark generations, on the contrary, remain heavy. Actually the top squark and sbottom squared masses can even be driven negative if the GUT-scale hierarchy $M^2_{\Phi_3} \ll M^2_{\Phi_{1,2}}$ is too pronounced, or if the gluino mass, whose contribution to the running of the squark masses tends to compensate for the two-loop gauge contribution, is too small.

The paper is organised in the following way. In the next section II, we introduce the concept of central diffractive production of SUSY Higgs bosons and top squarks; in II-A, the formalism of exclusive production and in II-B the experimental context are presented. In section III, we focus on the SUSY Higgs boson sector; in III-A, theoretical aspects of the Higgs boson spectrum and in III-B, the predictions for the LHC are displayed. In section IV, the case for top squark, and eventually bottom squark production is discussed; in IV-A, the theoretical framework, in IV-B, the predicted cross-sections and missing mass distribution and in IV-C, the top squark mass measurement by a threshold scan are given. The paper ended by a conclusion and outlook.

II. DIFFRACTIVE PRODUCTION OF SUSY HIGGS BOSON AND TOP SQUARKS

A. Exclusive central diffractive production

Let us introduce the model [1, 2, 4] we shall use for describing exclusive SUSY Higgs bosons and top squark pair production in double diffractive production. In [1, 2], the diffractive mechanism is based on two-gluon exchange between the two incoming protons. The soft pomeron is seen as a pair of gluons non-perturbatively coupled to the proton. One of the gluons is then coupled perturbatively to the hard process, either the SUSY Higgs bosons, or the $\tilde{t}\bar{\tilde{t}}$ pair, while the other one plays the rôle of a soft screening of colour, allowing for diffraction to occur. The corresponding cross-sections for Higgs bosons and $\tilde{t}\bar{\tilde{t}}$ production read:

$$
\begin{aligned}
d\sigma_h^{exc}(s) &= C_h \left(\frac{s}{M_h^2}\right)^{2\epsilon} \delta\left(\xi_1\xi_2 - \frac{M_h^2}{s}\right) \prod_{i=1,2} \left\{ d^2v_i \frac{d\xi_i}{1-\xi_i}\ \xi_i^{2\alpha' v_i^2} \exp(-2\lambda_h v_i^2) \right\} \sigma(gg \to h) \\
d\sigma_{\tilde{t}\bar{\tilde{t}}}^{exc}(s) &= C_{\tilde{t}\bar{\tilde{t}}} \left(\frac{s}{M_{\tilde{t}\bar{\tilde{t}}^2}}\right)^{2\epsilon} \delta^{(2)}\left(\sum_{i=1,2}(v_i + k_i)\right) \prod_{i=1,2} \left\{ d^2v_i d^2k_i d\xi_i\ d\eta_i\ \xi_i^{2\alpha' v_i^2} \exp(-2\lambda_{\tilde{t}\bar{\tilde{t}}} v_i^2) \right\} \sigma(gg \to \tilde{t}\bar{\tilde{t}}\ ) \qquad (5)
\end{aligned}
$$

where, in both equations, the variables v_i and ξ_i respectively denote the transverse momenta and fractional momentum losses of the outgoing protons. In the second equation, k_i and η_i are respectively the squark transverse momenta and rapidities. $\sigma(gg \to H), \sigma(gg \to \tilde{t}\bar{\tilde{t}}\ )$ are the hard production cross-sections which are given later on. The model normalisation constants $C_h, C_{\tilde{t}\bar{\tilde{t}}}$ are fixed from the fit to dijet diffractive production.

In the model, the soft pomeron trajectory is taken from the standard Donnachie-Landshoff parametrisation [54], namely $\alpha(t) = 1 + \epsilon + \alpha' t$, with $\epsilon \approx 0.08$ and $\alpha' \approx 0.25\mathrm{GeV}^{-2}$. $\lambda_h, \lambda_{\tilde{t}\bar{\tilde{t}}}$ are kept as in the original paper [1, 2] for the SM Higgs boson and $q\bar{q}$ pairs. Note that, in this model, the strong (non perturbative) coupling constant is fixed to a reference value $G^2/4\pi$, which will be taken from the fit to the observed centrally produced diffractive dijets.

In order to select exclusive diffractive states, it is required to take into account the corrections from soft hadronic scattering. Indeed, the soft scattering between incident particles tends to mask the genuine hard diffractive interactions at hadronic colliders. The formulation of this correction [24] to the scattering amplitudes $\mathcal{A}_{(H,\tilde{t}\bar{\tilde{t}})}$ consists in considering a gap survival probability (SP) function S such that

$$
\mathcal{A}(p_{T1}, p_{T2}, \Delta\Phi) = \{1 + \mathcal{A}_{SP}\} * \mathcal{A}_{(H,\tilde{t}\bar{\tilde{t}})} \equiv \mathcal{S} * \mathcal{A}_{(H,\tilde{t}\bar{\tilde{t}})} = \int d^2\mathbf{k}_T\ \mathcal{S}(\mathbf{k}_T)\ \mathcal{A}_{(H,\tilde{t}\bar{\tilde{t}}W)}(\mathbf{p}_{T1} - \mathbf{k}_T, \mathbf{p}_{T2} + \mathbf{k}_T)\ , \qquad (6)
$$

where $\mathbf{p}_{T1,2}$ are the transverse momenta of the outgoing $p, \bar{p}$ and $\Delta\Phi$ their azimuthal angle separation. $\mathcal{A}_{SP}$ is the soft scattering amplitude.

The correction factor is commonly evaluated to be of order 0.03 for the QCD exclusive diffractive processes at the LHC.

---

[2] In the following, we consider only top squarks. But the study remains unchanged for squarks (ie bottom squarks) if their masses is sufficiently low.

B. Experimental context

The DPEMC [25] Monte Carlo program provides an implementation of the Higgs boson, top squark and bottom squark pair production described above in both exclusive and inclusive double pomeron exchange modes. It uses HERWIG [26] as a cross-section library of hard QCD processes and, when required, convolutes them with the relevant pomeron fluxes and parton densities. The survival probabilities discussed in the previous section (0.03 for double pomeron exchange processes) have been introduced at the generator level. The cross sections at the generator level are given in the next section after this effect is taken into account.

A possible experimental setup for forward proton detection is described in detail in [4, 27]. We will only describe its main features here and discuss its relevance for the Higgs boson and top squark or bottom squark mass measurements.

In exclusive DPE or QED processes, the mass of the central heavy object can be reconstructed using the roman pot detectors and tagging both protons in the final state at the LHC. It is given by $M^2 = \xi_1 \xi_2 s$, where ξ_i are the proton fractional momentum losses, and s the total center-of-mass energy squared.

In the following, we assume the existence of two detector stations, located at ~ 210 m and ~ 420 m [27] from the interaction point. The ξ acceptance and resolution have been derived for each device using a complete simulation of the LHC beam parameters. The combined ξ acceptance is close to $\sim 60\%$ at low masses at about 100 GeV, and 90% at higher masses starting at about 220 GeV for ξ ranging from 0.002 to 0.1. In particular, this means that the low mass objects (Higgs bosons or top squarks) are mainly detected in the 420 m pots whereas the heavier ones in the closer pots at 210 m.

Our analysis does not assume any particular value for the ξ resolution. We will discuss in Sections III B and IV C how the resolution on the Higgs boson or the top squark quark masses depend on the detector resolutions, or in other words, the missing mass resolution.

III. SUSY HIGGS BOSON PRODUCTION

A. Theoretical aspects

Let us briefly recall the properties of the lightest MSSM Higgs boson h (for recent reviews, see Refs. [15] and [31]). As is well-known, h is constrained to be lighter than the Z boson at tree-level. Once radiative corrections are taken into account [32, 33, 34], the upper limit on its mass becomes $m_h \lesssim 135$ GeV. The actual value of m_h depends on several MSSM parameters: two parameters that are sufficient to describe the Higgs boson sector at tree-level, generally chosen to be m_A and $\tan\beta$, the ratio of the vevs of the two Higgs boson doublets of the MSSM; and additional parameters that control the size of the radiative corrections. These are the top squark and bottom squark soft supersymmetry breaking masses, assumed to be degenerate in this paper and denoted by M_{SUSY}, the top squark and bottom squark triscalar couplings (A-terms) A_t and A_b, and the supersymmetric Higgs boson mass parameter μ. The dependence of the lightest Higgs boson mass on these parameters can be roughly described as follows: m_h increases with m_A and $\tan\beta$, as well as with the common third generation squark mass M_{SUSY}. Its value also depends strongly on the top squark mixing parameter $X_t \equiv A_t - \mu \cot\beta$: starting from the "minimal mixing" $X_t = 0$, it increases with X_t and reaches a maximum for $X_t \approx \sqrt{6} M_S$, where $M_S^2 \equiv (m_{\tilde{t}_1}^2 + m_{\tilde{t}_2}^2)/2$ is the average of the two top squark squared masses ($M_S \simeq M_{SUSY}$ in the limit $M_{SUSY} \gg m_t$). This is illustrated by the following approximate formula for the one-loop upper bound on the lightest Higgs boson mass, valid in the decoupling limit $m_A \gg m_Z$ and for $m_t X_t \ll M_S^2$ [31, 35]:

$$m_h^2 \;\leq\; m_Z^2 \cos^2 2\beta + \frac{3 g^2 m_t^4}{8\pi^2 m_W^2} \left[\ln\left(\frac{M_S^2}{m_t^2}\right) + \frac{X_t^2}{M_S^2}\left(1 - \frac{X_t^2}{12 M_S^2}\right)\right]. \tag{7}$$

In the minimal mixing case, m_h can reach an upper limit of about 120 GeV for $M_{SUSY} \lesssim 1$ TeV, while it can reach about 135 GeV in the maximal mixing case [31].

The couplings of h can significantly depart from those of the SM Higgs boson. In particular, its tree-level couplings to down-type and up-type fermions (normalised to the SM Higgs boson couplings) are given by:

$$g_{hff} \;=\; \begin{cases} \sin(\beta-\alpha) + \cot\beta\, \cos(\beta-\alpha) & \text{(f = up-type fermion)} \\ \sin(\beta-\alpha) - \tan\beta\, \cos(\beta-\alpha) & \text{(f = down-type fermion)} \end{cases}, \tag{8}$$

where α is the angle that diagonalises the CP-even Higgs boson squared mass matrix and defines the physical CP-even states h and H. As for the couplings to the gauge bosons hZZ and hWW, they are suppressed by a factor $\sin(\beta-\alpha)$ relative to their SM values. In the decoupling regime $m_A \gg m_Z$ [12, 13], in which A, H and $H^\pm$ are

all much heavier than h, $|\cos(\beta-\alpha)| \leq \mathcal{O}(m_Z^2/m_A^2) \ll 1$ and therefore the couplings of the lightest MSSM Higgs boson h approach those of the SM Higgs boson (in particular, $g_{hff} \simeq 1$). On the contrary, in the case where $m_A \sim m_Z$ (or more precisely $m_A < m_h^{max}$, where m_h^{max} is the maximal value m_h can reach for fixed values of the squark parameters), $|\cos(\beta-\alpha)| \sim 1$ and therefore h has significantly different couplings from those of the SM Higgs boson. In particular, at large $\tan\beta$, in the so-called "anti-decoupling" regime [16], its couplings to down-type fermions are strongly enhanced ($|g_{hbb}| \simeq |g_{h\tau\tau}| \simeq \tan\beta \gg 1$), while its couplings to up-type fermions and gauge bosons are suppressed ($|g_{htt}| \sim \cot\beta \ll 1$ and $g_{hWW} = g_{hZZ} = \sin(\beta-\alpha) \ll 1$, in units of the SM Higgs boson couplings). As we shall see below, this enhances the production cross-section of the lightest Higgs boson via gluon fusion, while the associated production with gauge bosons, $q\bar{q} \to Zh/Wh$, is suppressed. Also the partial decay width of h into $b\bar{b}$ ($\tau^+\tau^-$), which is proportional to g_{hbb}^2 ($g_{h\tau\tau}^2$), is enhanced. By contrast, the decay $h \to \gamma\gamma$, which in the decoupling regime is dominated by the W boson loop, does not benefit from such an enhancement at large $\tan\beta$ (the subdominant bottom quark loop is enhanced, but the dominant W boson loop is suppressed), and has therefore a suppressed branching ratio in the antidecoupling regime. We close this short review of the antidecoupling regime by adding that the heavier CP-even Higgs boson H, contrary to h, has SM-like couplings, but it is much heavier than h and A. Finally, another regime of interest is the so-called "intense-coupling" regime [14], which occurs when $m_A \sim m_h^{max}$ and $\tan\beta$ is large. In this regime, all three neutral Higgs bosons are very close in mass, $m_h \approx m_A \approx m_H$, and have enhanced (suppressed) couplings to down-type fermions (down-type fermions and gauge bosons – the couplings AWW and AZZ are forbidden by CP invariance), so that it may be difficult to distinguish among them at the LHC.

Let us now discuss the MSSM lightest Higgs boson production via gluon fusion [36, 37, 38, 39, 40]. In the SM, the top quark loops give the main contribution to the cross-section, and the bottom loops give a smaller contribution. In the MSSM, the contribution of the bottom loops can become very large at large $\tan\beta$ (in the regime where the hbb couplings are enhanced) while the top quark loops are suppressed, resulting in an enhancement of the gluon fusion cross-section. In addition, top squark loops and (at large $\tan\beta$) bottom squark loops contribute. However, top squark loops significantly affect the cross-section only in the case of a light top squark, $m_{\tilde{t}_1} \lesssim (200-400)$ GeV. In the decoupling regime, their effects are particularly spectacular in the presence of a large top squark mixing, in which case they interfere destructively with the top quark contribution [41]. For bottom squark loops to be sizable, a large value of $\tan\beta$ is also needed, as well as a large value of $|\mu|$ in the decoupling regime. At leading order, the cross-section for h production via gluon fusion reads [42]:

$$\sigma(gg \to h) \;=\; \frac{G_F \alpha_S^2}{288\sqrt{2}\pi} \left| \frac{3}{4} \sum_q g_{hqq} A_q^h(\tau_q) + \frac{3}{4} \sum_{\tilde{q}} \frac{g_{h\tilde{q}\tilde{q}}}{m_{\tilde{q}}^2} A_{\tilde{q}}^h(\tau_{\tilde{q}}) \right|^2 \;, \tag{9}$$

where the loop functions $A_q^h(\tau)$ and $A_{\tilde{q}}^h(\tau)$ are given by:

$$A_q^h(\tau) \;=\; \frac{2}{\tau^2}\left[\tau + (\tau-1) f(\tau)\right], \qquad A_{\tilde{q}}^h(\tau) \;=\; \frac{1}{\tau^2}\left[f(\tau) - \tau\right], \tag{10}$$

$$f(\tau) \;=\; \begin{cases} \arcsin^2(\sqrt{\tau}) & \tau \leq 1 \\ -\frac{1}{4}\left[\ln\left(\frac{1+\sqrt{1-1/\tau}}{1-\sqrt{1-1/\tau}}\right) - i\pi\right]^2 & \tau > 1 \end{cases} , \tag{11}$$

and the parameters τ_q and $\tau_{\tilde{q}}$ are defined by $\tau_q \equiv m_h^2/4m_q^2$ and $\tau_{\tilde{q}} \equiv m_h^2/4m_{\tilde{q}}^2$, respectively. The couplings of h to quarks, g_{hqq}, are given by Eq. (8), and its couplings to the top squarks and the bottom squarks, $g_{h\tilde{t}_i\tilde{t}_i}$ and $g_{h\tilde{b}_i\tilde{b}_i}$ ($i = 1, 2$), by (in units of g/M_W):

$$g_{h\tilde{t}_1\tilde{t}_1} \;=\; -\left(\frac{1}{2}\cos^2\theta_{\tilde{t}} - \frac{2}{3}\sin^2\theta_W \cos 2\theta_{\tilde{t}}\right) M_Z^2 \sin(\beta+\alpha) + m_t^2 \frac{\cos\alpha}{\sin\beta} + \frac{1}{2}\sin 2\theta_{\tilde{t}}\, m_t \left(A_t \frac{\cos\alpha}{\sin\beta} + \mu \frac{\sin\alpha}{\sin\beta}\right), \tag{12}$$

$$g_{h\tilde{t}_2\tilde{t}_2} \;=\; -\left(\frac{1}{2}\cos^2\theta_{\tilde{t}} + \frac{2}{3}\sin^2\theta_W \cos 2\theta_{\tilde{t}}\right) M_Z^2 \sin(\beta+\alpha) + m_t^2 \frac{\cos\alpha}{\sin\beta} - \frac{1}{2}\sin 2\theta_{\tilde{t}}\, m_t \left(A_t \frac{\cos\alpha}{\sin\beta} + \mu \frac{\sin\alpha}{\sin\beta}\right), \tag{13}$$

$$g_{h\tilde{b}_1\tilde{b}_1} \;=\; \left(\frac{1}{2}\cos^2\theta_{\tilde{b}} - \frac{1}{3}\sin^2\theta_W \cos 2\theta_{\tilde{b}}\right) M_Z^2 \sin(\beta+\alpha) - m_b^2 \frac{\sin\alpha}{\cos\beta} + \frac{1}{2}\sin 2\theta_{\tilde{b}}\, m_b \left(-A_b \frac{\sin\alpha}{\cos\beta} + \mu \frac{\cos\alpha}{\cos\beta}\right), \tag{14}$$

$$g_{h\tilde{b}_2\tilde{b}_2} \;=\; \left(\frac{1}{2}\cos^2\theta_{\tilde{b}} + \frac{1}{3}\sin^2\theta_W \cos 2\theta_{\tilde{b}}\right) M_Z^2 \sin(\beta+\alpha) - m_b^2 \frac{\sin\alpha}{\cos\beta} - \frac{1}{2}\sin 2\theta_{\tilde{b}}\, m_b \left(-A_b \frac{\sin\alpha}{\cos\beta} + \mu \frac{\cos\alpha}{\cos\beta}\right), \tag{15}$$

where $\theta_{\tilde{t}}$ and $\theta_{\tilde{b}}$ are the mixing angle in the stop and the bottom squark sector respectively, defined by $\tilde{q}_1 = \cos\theta_{\tilde{q}}\, \tilde{q}_L + \sin\theta_{\tilde{q}}\, \tilde{q}_R$, $\tilde{q}_2 = -\sin\theta_{\tilde{q}}\, \tilde{q}_L + \cos\theta_{\tilde{q}}\, \tilde{q}_R$. In the regime we are interested in, which is characterised by a large value of

$\tan\beta$ and a suppressed value of $\sin(\beta-\alpha)$, there is no enhancement of $g_{h\tilde{t}_i\tilde{t}_i}$ at large top squark mixing, contrarily to what happens in the decoupling regime. However, $g_{h\tilde{b}_i\tilde{b}_i}$ is enhanced at large mixing; but this is compensated by the fact that $m_{\tilde{b}_1}$ and $m_{\tilde{b}_2}$ are generally larger than $m_{\tilde{t}_1}$ in typical MSSM scenarios. We therefore neglect the squark loops in the following discussion, although they are included in our numerical results. Neglecting as well the terms suppressed by $\cot\beta$, we then find the following enhancement factor for the MSSM cross-section with respect to the SM cross-section (the QCD corrections to the leading order cross sections are expected to reduce this ratio by some 30% at large $\tan\beta$ [15]):

$$\frac{\sigma_{MSSM}(gg\to h)}{\sigma_{SM}(gg\to h)} \;\approx\; \left|\sin(\beta-\alpha)-\tan\beta\cos(\beta-\alpha)\frac{A_b^h(\tau_b)}{A_t^h(\tau_t)+A_b^h(\tau_b)}\right|^2 . \tag{16}$$

We therefore expect a large enhancement factor at large values of $\tan\beta$ in the regime where $m_A < m_h^{max}$. This can indeed be seen in Fig. 1 (upper plot), where $\sigma_{MSSM}(gg\to h)/\sigma_{SM}(gg\to h)$ has been plotted as a function of m_h for $\tan\beta = 30$ and various values of the squark parameters. In the maximal mixing case, m_h^{max} is large and the antidecoupling condition $m_A < m_h^{max}$ is satisfied over the range $90\,\text{GeV} \le m_h \le 120\,\text{GeV}$ (remember that in this regime $m_h \approx m_A$), hence $\cos^2(\beta-\alpha)$ remains very close to 1, and the curve essentially reflects the dependence of the loop functions $A_t^h(\tau_t)$ and $A_b^h(\tau_b)$ on m_h. In the minimal mixing case, m_h^{max} is smaller, especially for $M_{SUSY} = 500$ GeV (namely $m_h^{max} \approx 114$ GeV for $M_{SUSY} = 1$ TeV, and $m_h^{max} \approx 107$ GeV for $M_{SUSY} = 500$ GeV), so that one leaves the anti-decoupling regime for much lower values of m_h than in the maximal mixing case. This explains why the enhancement factor strongly decreases when m_h approaches m_h^{max}, and finally reaches the decoupling regime value $\sigma_{MSSM}(gg\to h)/\sigma_{SM}(gg\to h) = 1$ for $m_h = m_h^{max}$ (up to squark loop effects, which remain small for the squark parameters considered here). Fig. 1 (lower plot) shows the dependence of the enhancement factor on $\tan\beta$ for $m_h = 100$ GeV. For this value of m_h, the condition $m_A < m_h^{max}$ is satisfied for all four sets of the squark parameters considered. For moderate values of $\tan\beta$ ($\tan\beta < 5$ is excluded experimentally for $m_h = 100$ GeV), the anti-decoupling regime is not yet reached, i.e. $\cos^2(\beta-\alpha)$ is large but not maximal ($\cos^2(\beta-\alpha) \sim 1$). For larger values of $\tan\beta$, say $\tan\beta \gtrsim 20$, the anti-decoupling regime is reached and the enhancement factor grows as $\tan^2\beta$, as expected.

B. SUSY Higgs boson production at the LHC

In this section, we consider the SUSY Higgs boson production for masses below 120 GeV when the Higgs boson decays into $b\bar{b}$, the least favourable case at the LHC. As mentioned in the previous section, Figure 1 shows the cross section enhancement factor for SUSY Higgs boson production with respect to the Standard Model case at generator level. In the upper plot of Fig. 1, the full and dashed lines show the results for the minimal mixing scenario for two SUSY masses respectively (1000 and 500 GeV) which lead to typical masses of the top squark and bottom squarks of 1010 or 520 GeV respectively. The cross section was computed using the bottom, top, top squark and bottom squark loops, while the effect of the top squark and bottom squark loops is less than one per mil. The enhancement factor can go up to a factor 20 compared to the Standard Model case, but is very dependent on the mass of the Higgs boson. In the maximal smearing scenario (dotted and dashed dotted curves in Fig. 1), the enhancement factor is found to be similar to that at low Higgs boson masses, but remains important at higher masses.

The bottom plot of Fig. 1 displays the dependence as a function of $\tan\beta$ for a Higgs boson mass of 100 GeV and for the same scenarii as before. The enhancement factor for the Higgs boson production cross section can reach a factor up to 45 for a value of $\tan\beta$ of 50. For this particular value of the mass of the Higgs boson, the model dependence is not very large.

It is important to note that we will benefit directly from the increase of the cross section since we will be looking for Higgs bosons decaying into $b\bar{b}$ in the main detector, and the branching ratio of $h\to b\bar{b}$ is quite stable as a function of the SUSY parameters in this region of phase space [3]. The diffractive search for SUSY Higgs boson production is thus the only one benefiting fully from the increase of the cross section at high values of $\tan\beta$.

In the following, we perform a detailed study of signal-over-background ratio in the case of a Higgs boson mass of 120 GeV. We chose this particular mass since most of the SUSY models predict a Higgs boson mass to be below this value, and this mass leads to the worst favourable scenario (the lowest cross section and signal-over-background ratios) with respect to lower masses. In Fig. 2, we give the signal-over-background ratio for Standard Model and

[3] This is not the case when one looks into non diffractive SUSY Higgs bosons decaying into $\gamma\gamma$ which is strongly suppressed at high $\tan\beta$, see paragraph III A.

SUSY Higgs boson production for a mass of the Higgs boson of 120 GeV and for different values of $\tan\beta$, as a function of the roman pot (Higgs boson) mass resolution for a luminosity of 100 fb^{-1}. This study was performed after a fast simulation of the CMS detector (the ATLAS detector simulation is expected to produce very similar results) and the following experimental cuts.

First of all, we require both protons in the final state to be detected in the roman pot detectors, and we take into account the acceptance of these detectors as it is discussed in section I. The cuts used in the analysis are detailed in Ref. [3]. The basic idea is to require two high p_T b-jets with $p_{T1} > 45$ GeV, $p_{T2} > 30$ GeV, coming from the decay of the Higgs boson in $b\bar{b}$ at low masses. The difference in azimuth between the two jets should be $170 < \Delta\Phi < 190$ degrees, asking the jets to be back-to-back. Both jets are required to be central, $|\eta| < 2.5$, b-tagged, with the difference in rapidity of both jets satisfying $|\Delta\eta| < 0.8$. A cut is applied on the ratio of the dijet mass to the total mass of all jets measured in the calorimeters, $M_{JJ}/M_{all} > 0.75$. The ratio of the dijet mass to the missing mass should fulfil $M_{JJ}/(\xi_1\xi_2 s)^{1/2} > 0.8$.

The case for the Standard Model Higgs boson was already given in [3], and we follow the same approach concerning the background and signal studies. To compute the signal over background ratios, both signals and backgrounds dominated by exclusive $b\bar{b}$ production have been integrated over a 2 GeV mass window. After cuts, the typical number of events expected for the signal of a 120 GeV Higgs boson and for a luminosity of 100 fb^{-1} is 27.1, 73.2, 154, 398 and 1198 for Standard Model and SUSY ($\tan\beta$= 15, 20, 30 and 50) Higgs boson production respectively. If the Higgs boson is supersymmetric and is produced with a large value of $\tan\beta$, the diffractive production of SUSY Higgs bosons could lead to a discovery in the double pomeron exchange mode at the LHC. We notice in Fig. 2 that the signal over background can reach a value up to 54, 26, 16, and 13 for respective Higgs boson mass resolutions in roman pot detectors of 1, 2, 3 and 4 GeV and for a value of $\tan\beta$ of 50 for a luminosity of 100 fb^{-1}.

IV. PRODUCTION OF TOP (BOTTOM) SQUARK PAIRS

A. Theoretical framework

In the MSSM, for each quark flavour q, there are two supersymmetric scalar partners $\tilde{q}_L$ and $\tilde{q}_R$ associated with the two fermion chiralities q_L and q_R. These scalars are not mass eigenstates in general, due to the presence of soft supersymmetry breaking terms which mix them, the A-terms $A_q y_q \tilde{Q}_L \tilde{q}_R^\star H + \text{h.c.}$, where y_q is the Yukawa coupling of the quark q and H is one of the two MSSM Higgs boson doublet. The mass eigenstates $\tilde{q}_1$ and $\tilde{q}_2$ are obtained by diagonalising the following 2×2 matrix [43]:

$$\begin{pmatrix} M_Q^2 + m_q^2 + D_L & m_q X_q \\ m_q X_q & M_R^2 + m_q^2 + D_R \end{pmatrix}, \tag{17}$$

where $D_L \equiv (T_q^3 - Q_q \sin^2\theta_W) m_Z^2 \cos 2\beta$, $D_R \equiv Q_q \sin^2\theta_W m_Z^2 \cos 2\beta$, $X_q \equiv A_q - \mu \cot\beta$ for up-type squarks and $X_q \equiv A_q - \mu \tan\beta$ for down-type squarks. The soft supersymmetry breaking squark masses M_Q and M_R are of the order of the supersymmetry breaking scale M_{SUSY}, and phenomenological constraints require the A-term parameter A_q to be at most a few M_{SUSY} [44]. Neglecting the terms proportional to m_Z^2 in the squark mass matrix, the mass eigenvalues and the mixing angle which relates the weak interaction eigenstates $\tilde{q}_{L,R}$ to the mass eigenstates $\tilde{q}_{1,2}$ are given by the following expressions:

$$m^2_{\tilde{q}_{1,2}} \;=\; \frac{1}{2}\left(M_Q^2 + M_R^2 + m_q^2 \mp \sqrt{(M_Q^2 - M_R^2)^2 + 4 m_q^2 X_q^2}\right), \qquad \tan\theta_{\tilde{q}} \;=\; \frac{2 m_q X_q}{M_Q^2 - M_R^2}\,. \tag{18}$$

In practise, the mixing is significant only if $m_q X_q \sim M^2_{SUSY}$, which can happen for the top squark and, at large $\tan\beta$, for the bottom squark. In this case, one can have a strong hierarchy between the two mass eigenstates, $m_{\tilde{q}_1} \ll m_{\tilde{q}_2}$. The 95% C.L. experimental bounds on the lightest top squark and bottom squark masses are $m_{\tilde{t}_1} > 95.7$ GeV and $m_{\tilde{b}_1} > 89$ GeV, respectively, while the bound on the other squarks is 250 GeV [45] (the latter bound also applies to $\tilde{b}_1$ if mixing effects are small in the bottom squark sector). Although these bounds where derived under specific assumptions and may therefore not hold in some regions of the MSSM parameter space, they are rather robust.

In our experimental study, we consider the following values for the lightest top squark mass: 174.3 GeV (i.e. $m_{\tilde{t}_1} = m_t$), 210 GeV and 393 GeV. As we shall see, the resolution that can be obtained on the top squark mass crucially depends on its decay width, which in turn is a function of the top squark mass and of the other MSSM parameters. If the top squark is very light, it is likely to be the next-to-lightest supersymmetric particle, assuming the lightest supersymmetric particle (LSP) is the lightest neutralino $\tilde{\chi}_1^0$. Then all two-body decay channels occurring at the tree level are closed. If in addition the tree-body decay channels $\tilde{t}_1 \to bW^+\tilde{\chi}_1^0$ and $\tilde{t}_1 \to bH^+\tilde{\chi}_1^0$ are not

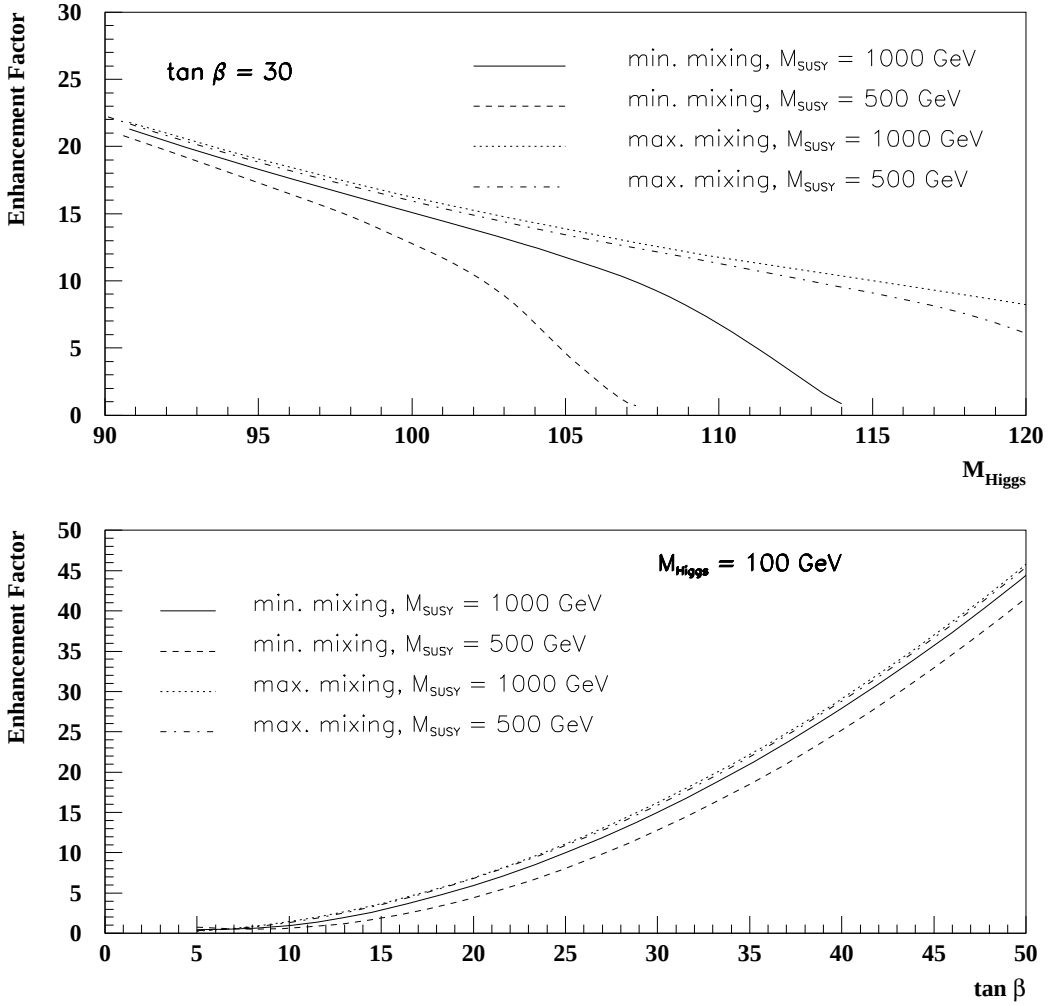

FIG. 1: Enhancement factor for the diffractive Higgs boson production cross section. Upper plot: enhancement factor as a function of the Higgs boson mass for a value of $\tan\beta = 30$, and different mixing scenarii and $SUSY$ masses (full line: minimal mixing, $M_{SUSY} = 1000$ GeV, dashed line: minimal mixing, $M_{SUSY} = 500$ GeV, dotted line: maximal mixing, $M_{SUSY} = 1000$ GeV, dashed dotted line: maximal mixing, $M_{SUSY} = 500$ GeV. Lower plot: similar study as a function of $\tan\beta$ for a Higgs boson mass of 100 GeV.

kinematically accessible, the main decay mode is expected to be the loop-induced flavour violating decay $\tilde{t}_1 \to c\tilde{\chi}_1^0$ [46]. The decay width of the lightest top squark is then given by [46]:

$$\Gamma(\tilde{t}_1 \to c\tilde{\chi}_1^0) \;=\; \frac{g^2}{16\pi}|f_{L1}^c|^2|\epsilon|^2 m_{\tilde{t}_1}\left(1-\frac{m_{\tilde{\chi}_1^0}^2}{m_{\tilde{t}_1}^2}\right)^2 \;, \tag{19}$$

where $|f_{L1}^c| \leq 1$ is the $\tilde{c}_L$-c_L-$\tilde{\chi}_1^0$ coupling, and ϵ is a flavour-violating insertion. The authors of Ref. [46] estimated $|\epsilon| \sim (1-4)\times 10^{-4}$ in mSUGRA, yielding $\Gamma(\tilde{t}_1 \to c\tilde{\chi}_1^0) \lesssim (0.085-1.4)\times 10^{-9}\, m_{\tilde{t}_1}[1-(m_{\tilde{\chi}_1^+}/m_{\tilde{t}_1})^2]^2$; but depending on the mSUGRA parameters $|\epsilon|$ could be either much smaller or larger, in particular at large $\tan\beta$ where $|\epsilon|$ behaves like $\tan^2\beta$. In non-minimal SUGRA models, $|\epsilon|$ could even be of order one. However, in the regions of the MSSM parameter space where $\Gamma(\tilde{t}_1 \to c\tilde{\chi}_1^0)$ is suppressed, the four-body decay modes $\tilde{t}_1 \to b\tilde{\chi}_1^0 f\bar{f}$ are likely to be dominant [47, 48]. For larger top squark masses, the three-body decay channels $\tilde{t}_1 \to bW^+\tilde{\chi}_1^0$ and $\tilde{t}_1 \to bH^+\tilde{\chi}_1^0$ [49, 50] (and, if the sleptons are lighter than the lightest top squark, $\tilde{t}_1 \to b\,\nu_l\,\tilde{l}^+$ and $\tilde{t}_1 \to b\,\tilde{\nu}_l\,l^+$ [46, 50, 51]) open up and tend to

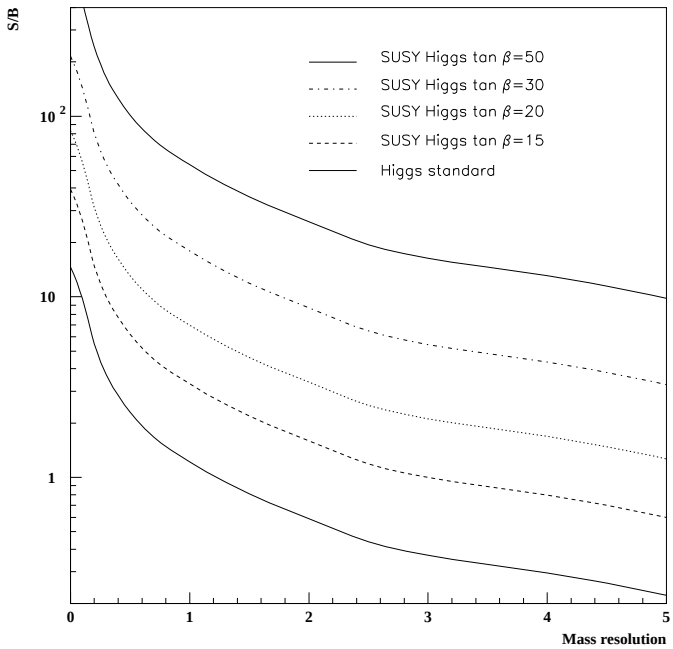

FIG. 2: Signal over background as a function of roman pot mass resolution for a Higgs boson mass of 120 GeV and for different values of $\tan\beta$. From bottom to top: full line: Standard Model Higgs boson, dashed line: SUSY Higgs boson with $\tan\beta$ =15, dotted line: $\tan\beta$ =20, dashed dotted line: $\tan\beta$ =30, full line: $\tan\beta$ =50.

dominate. Finally, when $m_{\tilde{t}_1} > m_b + m_{\tilde{\chi}_1^+}$ and $m_{\tilde{t}_1} > m_t + m_{\tilde{\chi}_1^0}$, the two-body decays $\tilde{t}_1 \to b\tilde{\chi}_1^+$ and $\tilde{t}_1 \to t\tilde{\chi}_1^0$ become kinematically accessible and dominate the lightest top squark decays[4] [52]. The partial decay width of $\tilde{t}_1 \to b\tilde{\chi}_1^+$ is given by:

$$\Gamma(\tilde{t}_1 \to b\tilde{\chi}_1^+) \;=\; \frac{g^2}{16\pi}\,(l_{11}^2 + k_{11}^2)\, m_{\tilde{t}_1} \left(1 - \frac{m_{\tilde{\chi}_1^+}^2}{m_{\tilde{t}_1}^2}\right)^2 \;, \tag{20}$$

where l_{11} and k_{11} are chargino couplings. Since $|l_{11}|$, $|k_{11}| \lesssim 1$, $\Gamma(\tilde{t}_1 \to b\tilde{\chi}_1^+) \lesssim 0.0085\, m_{\tilde{t}_1}[1 - (m_{\tilde{\chi}_1^+}/m_{\tilde{t}_1})^2]^2$. The decay $\tilde{t}_1 \to t\tilde{\chi}_1^0$ has a larger phase space suppression.

For our experimental study, we do not consider any specific benchmark scenario, but simply assume $m_{\tilde{t}_1} < m_{\tilde{\chi}_1^+}$ for the cases $m_{\tilde{t}_1} = 174$ and 210 GeV. Then we conservatively take $\Gamma_{\tilde{t}_1} = 100$ MeV for $m_{\tilde{t}_1} = 174$ and 210 GeV, although the actual decay width could be much smaller. For $m_{\tilde{t}_1} = 393$ GeV, we assume that the two-body decay $\tilde{t}_1 \to b\tilde{\chi}_1^+$ is accessible, and we take the decay width computed for SPS 1a, $\Gamma_{\tilde{t}_1} = 1.8$ GeV [19].

B. Stop production cross section and missing mass distribution

At hadron colliders, top squarks can be produced at lowest QCD order via quark-antiquark annihilation and gluon-gluon fusion. In the present study, we are interested in the $J_z = 0$, colour-singlet gluon-gluon fusion cross-section; it reads, at the parton level [53]:

$$\frac{d\sigma_{LO}}{dt}(gg \to \tilde{t}_i\bar{\tilde{t}}_i) \;=\; \frac{4\pi}{12}\frac{\alpha_s^2}{s^2}\frac{m_{\tilde{t}_i}^4}{E_T^4} \tag{21}$$

[4] We do not consider the decays $\tilde{t}_1 \to t\tilde{g}$ and $\tilde{t}_1 \to \tilde{b}_i W^+$, $\tilde{b}_i H^+$, since the gluinos and the other squarks are generally heavier than the lightest top squark.

where $\sqrt{s}$ is the invariant energy of the subprocess, $m_{\tilde{t}_i}$ is the top squark mass, and E_T is the transverse energy of the final particles.

The top squark production cross section has been obtained using the DPEMC generator [25] after applying a survival probability of 0.03. The top squark pair production cross section as a function of the top squark mass is given in Fig. 3. The $\tilde{t}\bar{\tilde{t}}$ production cross section is found to be 26.3, 14.1 and 1.1 fb for a top squark mass of 174.3 (at about the top quark mass), 210 and 393 GeV respectively.

The distribution of the missing mass distribution for $t\bar{t}$ and $\tilde{t}\bar{\tilde{t}}$ events for $m_{\tilde{t}} = m_t$ =174.3 GeV is shown in Fig. 4 for a luminosity of 100 fb^{-1}. The missing mass distribution for top squark (top) events is in full (dashed) line. The cross-section rise at threshold is much faster than for top quarks and typical of pair production of scalar particles. The exploitation of this threshold to measure the stop quark mass is studied in the next section : the idea is to perform a kind of threshold scan of the $\tilde{t}\bar{\tilde{t}}$ production cross section by measuring the missing mass using the roman pot detectors.

C. Stop mass measurement

In this section, we describe briefly the method we used to obtain the stop mass resolution and its results. The histogram method [5] is described in more detail in Ref. [29]. It corresponds to the comparison of the mass distribution in data with some reference distributions following a Monte Carlo simulation of the detector with different input masses corresponding to the data luminosity. As an example, we can produce a data sample for 100 fb^{-1} with a top squark mass of 210 GeV, and a few MC samples corresponding to top squark masses between 180 and 240 GeV by steps of 1 GeV. To evaluate the statistical uncertainty due to the method itself, we perform the fits with some 100 different "data" ensembles. For each ensemble, one obtains a different reconstructed top squark mass, the dispersion corresponding only to statistical effects. The χ^2 is defined using the approximation of poissonian errors as given in Ref. [30]. Each ensemble thus gives a χ^2 curve which in the region of the minimum is fitted with a fourth-order polynomial. The position of the minimum of the polynomial gives the best value of the top squark mass and the uncertainty $\sigma(m_{\tilde{t}}$ is obtained from the values where $\chi^2 = \chi^2_{\rm min} + 1$.

The results are given in Fig. 5 and 6. Fig. 5 displays the results on the top squark mass resolution for a top squark mass of 210 GeV as an example, as a function of luminosity, for different roman pot resolutions. We notice that the results depend only weakly on the roman pot resolution and mostly on the number of events produced for a given luminosity. The resolution on the top squark mass is thus dominated by statistics. We should also note that the integrated luminosity does not take into account the efficiency of the cuts to select the $\tilde{t}\bar{\tilde{t}}$ events since these efficiencies depend strongly on the SUSY parameters. A typical efficiency of 60% is found requesting a missing transverse energy to be greater than 80 GeV, and either two reconstructed jets or one lepton and one jet with a transverse momentum greater than 20 GeV. In Fig. 6, we display the resolution obtained for the three values of the top squark mass discussed above. We notice that we obtain a resolution of about 0.4, 0.7 and 4.3 GeV for a top squark mass of 174.3, 210 and 393 GeV for a luminosity (divided by the signal efficiency) of 100 fb^{-1}. As it was mentionned in paragraph IV A, the top squark width has been taken into account in this study. For a top squark mass of 174.3, 210 GeV, the top squark width of 100 MeV has a negligible effect, whereas the top squark width of 1.8 GeV for a top squark mass of 393 GeV cannot be neglected.

V. CONCLUSION AND OUTLOOK

In this paper, we described the adavantages of diffractive SUSY particle productions for two different processes, namely the SUSY Higgs bosons and top squark pairs. The diffractive SUSY Higgs boson production cross section is noticeably enhanced athigh values of $\tan\beta$ and since we look for Higgs boson decaying into $b\bar{b}$, it is possible to benefit directly from the enhancement of the cross section contrary to the non diffractive case. A signal-over-background up to a factor 50 can be reached for 100 fb^{-1} for $\tan\beta \sim 50$. In particular, we analyze in detail the *antidecoupling* regime, in which H behaves like the SM Higgs boson, while h has enhanced (resp. suppressed) couplings to down-type fermions (resp. up-type fermions and gauge bosons). We find that central diffraction production seems to be promising in that regime.

---

[5] In Ref. [29], we give two methods to measure the W boson or the top mass, namely the histogram or the turn-on fit methods. For a matter of simplicity, we used only the histogram method in this paper.

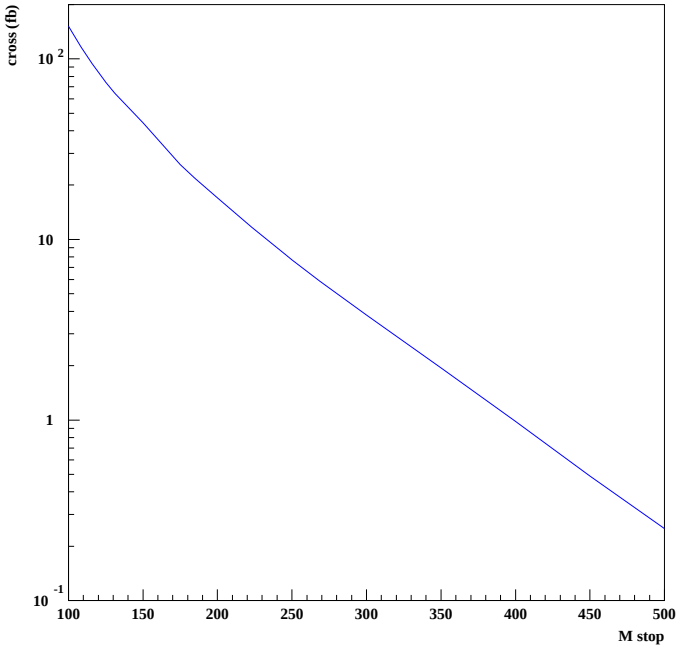

FIG. 3: Top squark pair production cross section as a function of the top squark mass.

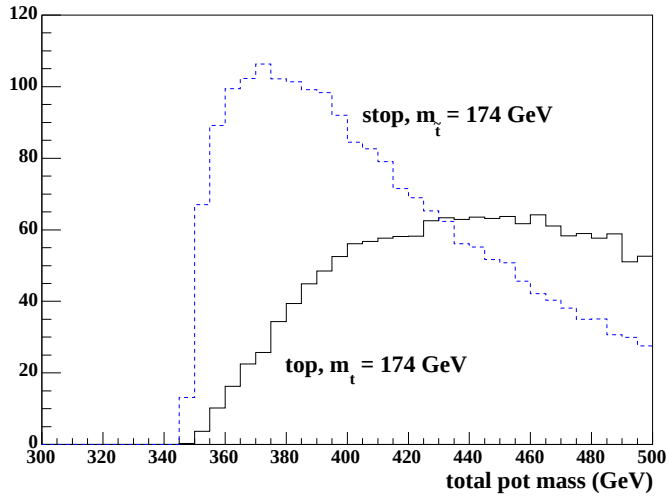

FIG. 4: Distribution of the missing mass for 100 fb^{-1} for $t\bar{t}$ events (dashed line), and for $\tilde{t}\bar{\tilde{t}}$ (full line) for $m_{top} = m_{\tilde{t}}$. The faster rise of the stop quark cross-section as a function of missing mass is due to the scalar nature of these particles.

The other application is to use the so-called "threshold-scan method" to measure the top squark mass in *exclusive* events. The idea is quite simple: one measures the turn-on point in the missing mass distribution above twice the top squark mass. After taking into account the top squark width, we obtain a resolution on the top squark mass of 0.4, 0.7 and 4.3 GeV for a top squark mass of 174.3, 210 and 393 GeV for a luminosity (divided by the signal efficiency) of 100 fb^{-1}. We notice that we reach typical mass resolutions which can be obtained at a linear collider. The process is thus similar to those at linear colliders (all final states are detected) without the initial state radiation problem.

It should be once more stressed that production via the diffractive exclusive processes (1) is model dependent, and definitely needs the Tevatron data to test the models. It will allow to determine more precisely the production cross section by testing and measuring at the Tevatron the jet and photon production for high masses and high dijet or

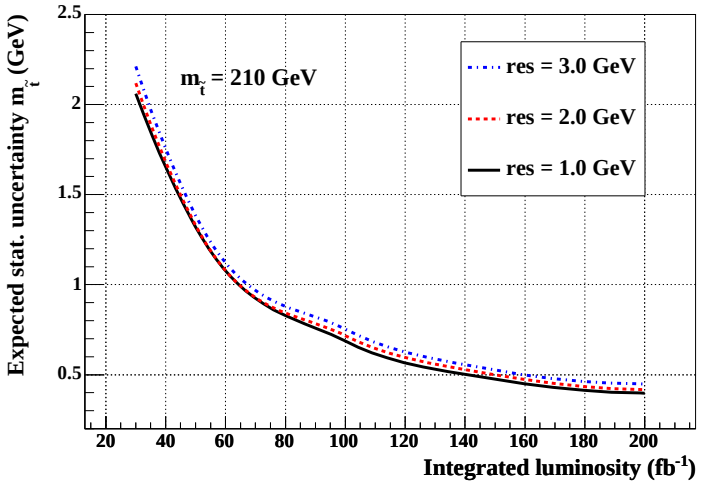

FIG. 5: Expected statistical precision of the $\tilde{t}$ mass as a function of the integrated luminosity for various resolutions of the roman pot detectors using the histogram-fitting method.

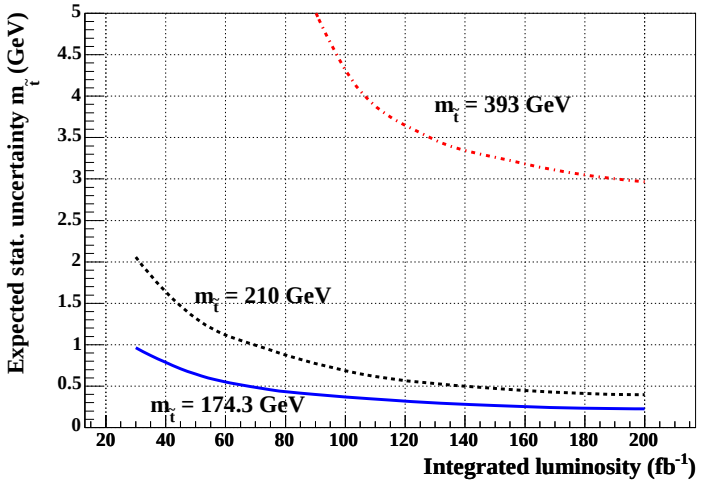

FIG. 6: Expected statistical precision of the $\tilde{t}$ mass as a function of the integrated luminosity for different $\tilde{t}$ masses (174.3, 210 and 393 GeV).

diphoton mass fraction.

On the other hand, it is also possible to perform a similar study using *inclusive* double pomeron exchanges (2). These processes have already been observed by many experiments but suffer from the lack of knowledge on the gluon density inthe pomeron at high β. The first step is thus to measure this gluon density by, for instance, using dijet events or the threshold scan method for inclusive $t\bar{t}$ production. Once the high-β gluon better determined, it is possible to look for top squark events using again the threhold scan method and deviation at high masses provided the cross section is high enough. This study goes beyond the purpose of the present paper but certainly deserves a dedicated study [63].

VI. ACKNOWLEDGMENTS

We thank Pavel Demine for his participation to this study at an early stage and for useful discussions.

---

[1] A. Bialas, P. V. Landshoff, *Phys. Lett.* **B256** (1990) 540.
[2] A. Bialas, W. Szeremeta, *Phys. Lett.* **B296** (1992) 191;
A. Bialas, R. Janik, *Zeit. für. Phys.* **C62** (1994) 487.
[3] M. Boonekamp, R. Peschanski and C. Royon, Phys. Lett. B **598**, 243 (2004) [arXiv:hep-ph/0406061].
[4] M. Boonekamp, R. Peschanski, C. Royon, *Phys. Rev. Lett.* **87** (2001) 251806;
M. Boonekamp, A. De Roeck, R. Peschanski, C. Royon, *Phys. Lett.* **B550** (2002) 93;
M. Boonekamp, R. Peschanski, C. Royon, *Nucl. Phys.* **B669** (2003) 277, Err-ibid **B676** (2004) 493;
for a general review see C. Royon, *Mod. Phys. Lett.* **A18** (2003) 2169.
[5] B. Cox, J. Forshaw, B. Heinemann, *Phys. Lett.* **B540** (2002) 263.
[6] R. Enberg, G. Ingelman, A. Kissavos, N. Timneanu, *Phys. Rev. Lett.* **89** (2002) 081801.
[7] V.A. Khoze, A.D. Martin, M.G. Ryskin, *Eur. Phys. J.* **C19** (2001) 477, Err-ibid **C20** (2001) 599;
V.A. Khoze, A.D. Martin, M.G. Ryskin, *Eur. Phys. J.* **C23** (2002) 311;
V.A. Khoze, A.D. Martin, M.G. Ryskin, *Eur. Phys. J.* **C24** (2002) 581.
[8] J.D. Bjorken, *Phys. Rev.* **D47** (1993) 101;
J.R. Cudell, O.F. Hernandez, *Nucl. Phys.* **B471** (1996) 471;
E.M. Levin, hep-ph/9912403 and references therein;
J. Pumplin, *Phys. Rev.* **D52** (1995) 1477;
A. Berera and J.C. Collins, *Nucl. Phys.* **474** (1996) 183.
[9] M.G. Albrow and A. Rostovtsev, hep-ph/0009336.
[10] D. Goulianos, talk given at the workshop on Diffraction at the LHC, Rio de Janeiro, March 31 - April 2 2004; M. Gallinaro [CDF - Run II Collaboration], [arXiv:hep-ph/0505159].
[11] For recent reviews of supersymmetry and the MSSM, see e.g. S. P. Martin, [arXiv:hep-ph/9709356]; D. J. H. Chung, L. L. Everett, G. L. Kane, S. F. King, J. Lykken and L. T. Wang, Phys. Rep. **407** (2005) 1 [arXiv:hep-ph/0312378]; I. J. R. Aitchison, [arXiv:hep-ph/0505105].
[12] H. E. Haber and Y. Nir, Phys. Lett. B **306** (1993) 327 [arXiv:hep-ph/9302228]; H. E. Haber, [arXiv:hep-ph/9505240].
[13] J. F. Gunion and H. E. Haber, Phys. Rev. D **67** (2003) 075019 [arXiv:hep-ph/0207010].
[14] E. Boos, A. Djouadi, M. Muhlleitner and A. Vologdin, Phys. Rev. D **66** (2002) 055004 [arXiv:hep-ph/0205160]; E. Boos, A. Djouadi and A. Nikitenko, Phys. Lett. B **578** (2004) 384 [arXiv:hep-ph/0307079].
[15] A. Djouadi, [arXiv:hep-ph/0503173].
[16] See e.g. J. F. Gunion, A. Stange and S. Willenbrock, [arXiv:hep-ph/9602238].
[17] A. B. Kaidalov, V. A. Khoze, A. D. Martin and M. G. Ryskin, Eur. Phys. J. C **31** (2003) 387 [arXiv:hep-ph/0307064].
[18] A. H. Chamseddine, R. Arnowitt and P. Nath, Phys. Rev. Lett. **49** (1982) 970; R. Barbieri, S. Ferrara and C. A. Savoy, Phys. Lett. B **119**, 343 (1982); L. J. Hall, J. Lykken and S. Weinberg, Phys. Rev. D **27** (1983) 2359.
[19] N. Ghodbane and H. U. Martyn, in *Proc. of the APS/DPF/DPB Summer Study on the Future of Particle Physics (Snowmass 2001)* ed. N. Graf, [arXiv:hep-ph/0201233]
[20] N. Ghodbane, [arXiv:hep-ph/9909499].
[21] M. Battaglia, A. De Roeck, J. R. Ellis, F. Gianotti, K. A. Olive and L. Pape, Eur. Phys. J. C **33** (2004) 273 [arXiv:hep-ph/0306219].
[22] M. Drees, Phys. Rev. D **33** (1986) 1468; S. Dimopoulos and G. F. Giudice, Phys. Lett. B **357** (1995) 573 [arXiv:hep-ph/9507282]; A. Pomarol and D. Tommasini, Nucl. Phys. B **466** (1996) 3 [arXiv:hep-ph/9507462]; A. G. Cohen, D. B. Kaplan and A. E. Nelson, Phys. Lett. B **388**, 588 (1996) [arXiv:hep-ph/9607394].
[23] N. Arkani-Hamed and H. Murayama, Phys. Rev. D **56** (1997) 6733 [arXiv:hep-ph/9703259].
[24] A. Kupco, C. Royon and R. Peschanski, Phys. Lett. B **606**, 139 (2005) [arXiv:hep-ph/0407222]. A. Kupco, R. Peschanski, C. Royon, hep-ph/0407222.
[25] M. Boonekamp, T. Kucs, *Comput. Phys. Commun.* **167** (2005) 217.
[26] G. Corcella et al., *JHEP* **0101:010** (2001).
[27] J. Kalliopuska, T. Mäki, N. Marola, R. Orava, K. Österberg, M. Ottela, HIP-2003-11/EXP.
[28] CMSIM, fast simulation of the CMS detector, CMS Collab., Technical Design Report (1997);
TOTEM Collab., Technical Design Report, CERN/LHCC/99-7;
ATLFAST, fast simulation of the ATLAS detector, ATLAS Collab, Technical Design Report, CERN/LHC C/99-14.
[29] M. Boonekamp, J. Cammin, R. Peschanski and C. Royon, [arXiv:hep-ph/0504199].
[30] N. Gehrels, Astrophys. J. **303**, 336 (1986).
[31] M. Carena and H. E. Haber, Prog. Part. Nucl. Phys. **50** (2003) 63 [arXiv:hep-ph/0208209].
[32] Y. Okada, M. Yamaguchi and T. Yanagida, Prog. Theor. Phys. **85**, 1 (1991).
[33] J. R. Ellis, G. Ridolfi and F. Zwirner, Phys. Lett. B **257** (1991) 83.
[34] H. E. Haber and R. Hempfling, Phys. Rev. Lett. **66**, 1815 (1991).

[35] H. E. Haber, R. Hempfling and A. H. Hoang, Z. Phys. C **75** (1997) 539 [arXiv:hep-ph/9609331].
[36] J. F. Gunion and H. E. Haber, Nucl. Phys. B **278** (1986) 449.
[37] A. Djouadi, M. Spira and P. M. Zerwas, Phys. Lett. B **264**, 440 (1991).
[38] S. Dawson, Nucl. Phys. B **359** (1991) 283.
[39] M. Spira, A. Djouadi, D. Graudenz and P. M. Zerwas, Nucl. Phys. B **453**, 17 (1995) [arXiv:hep-ph/9504378].
[40] S. Dawson, A. Djouadi and M. Spira, Phys. Rev. Lett. **77** (1996) 16 [arXiv:hep-ph/9603423].
[41] A. Djouadi, Phys. Lett. B **435**, 101 (1998) [arXiv:hep-ph/9806315].
[42] J. F. Gunion, H. E. Haber, G. L. Kane and S. Dawson, *"The Higgs Hunter's Guide"*, Addison-Wesley, Reading (USA), 1990.
[43] J. R. Ellis and S. Rudaz, Phys. Lett. B **128** (1983) 248; M. Drees and K. I. Hikasa, Phys. Lett. B **252**, 127 (1990).
[44] J. M. Frere, D. R. T. Jones and S. Raby, Nucl. Phys. B **222**, 11 (1983); H. P. Nilles, M. Srednicki and D. Wyler, Phys. Lett. B **120** (1983) 346; J. P. Derendinger and C. A. Savoy, Nucl. Phys. B **237**, 307 (1984).
[45] S. Eidelman *et al.* [Particle Data Group], Phys. Lett. B **592** (2004) 1.
[46] K. I. Hikasa and M. Kobayashi, Phys. Rev. D **36** (1987) 724.
[47] C. Boehm, A. Djouadi and Y. Mambrini, Phys. Rev. D **61** (2000) 095006 [arXiv:hep-ph/9907428].
[48] A. Djouadi, M. Guchait and Y. Mambrini, Phys. Rev. D **64** (2001) 095014 [arXiv:hep-ph/0105108].
[49] W. Porod and T. Wohrmann, Phys. Rev. D **55** (1997) 2907 [Erratum-ibid. D **67** (2003) 059902] [arXiv:hep-ph/9608472].
[50] W. Porod, Phys. Rev. D **59**, 095009 (1999) [arXiv:hep-ph/9812230].
[51] A. Datta, M. Guchait and K. K. Jeong, Int. J. Mod. Phys. A **14** (1999) 2239 [arXiv:hep-ph/9903214].
[52] For reviews of the two-body decays of the lightest top squark, see e.g. W. Porod, [arXiv:hep-ph/9804208]; S. Kraml, [arXiv:hep-ph/9903257].
[53] V.A. Khoze, A.D. Martin, M.G. Ryskin, *Eur. Phys. J.* **C23** (2002) 311.
[54] A. Donnachie, P.V. Landshoff, *Phys. Lett.* **B296** (1992) 227.
[55] A. Bzdak, *Acta Phys. Polon.* **B35** (2004) 1733.
[56] L. Lonnblad, M. Sjodahl, *JHEP* **0402:042** (2004).
[57] V.A. Khoze, A.D. Martin, M.G. Ryskin, *Eur. Phys. J.* **C18** (2000) 167.
[58] A. Bialas, *Acta Phys. Pol.* **B33** (2002) 26.
[59] A. Bialas, R. Peschanski, *Phys. Lett.* **B575** (2003) 30.
[60] T. Sjostrand, P. Eden, C. Friberg, L. Lonnblad, G. Miu, S. Mrenna, E. Norrbin, *Comput. Phys. Commun.* **135** (2001) 238.
[61] M.G. Albrow, A. Rostovtsev, hep-ph/0009336.
[62] A. De Roeck, V.A. Khoze, A.D. Martin, M.G. Ryskin, R. Orava, *Eur. Phys. J.* **C25** (2002) 391.
[63] M. Boonekamp, J. Cammin, R. Peschanski and C. Royon, to be published.

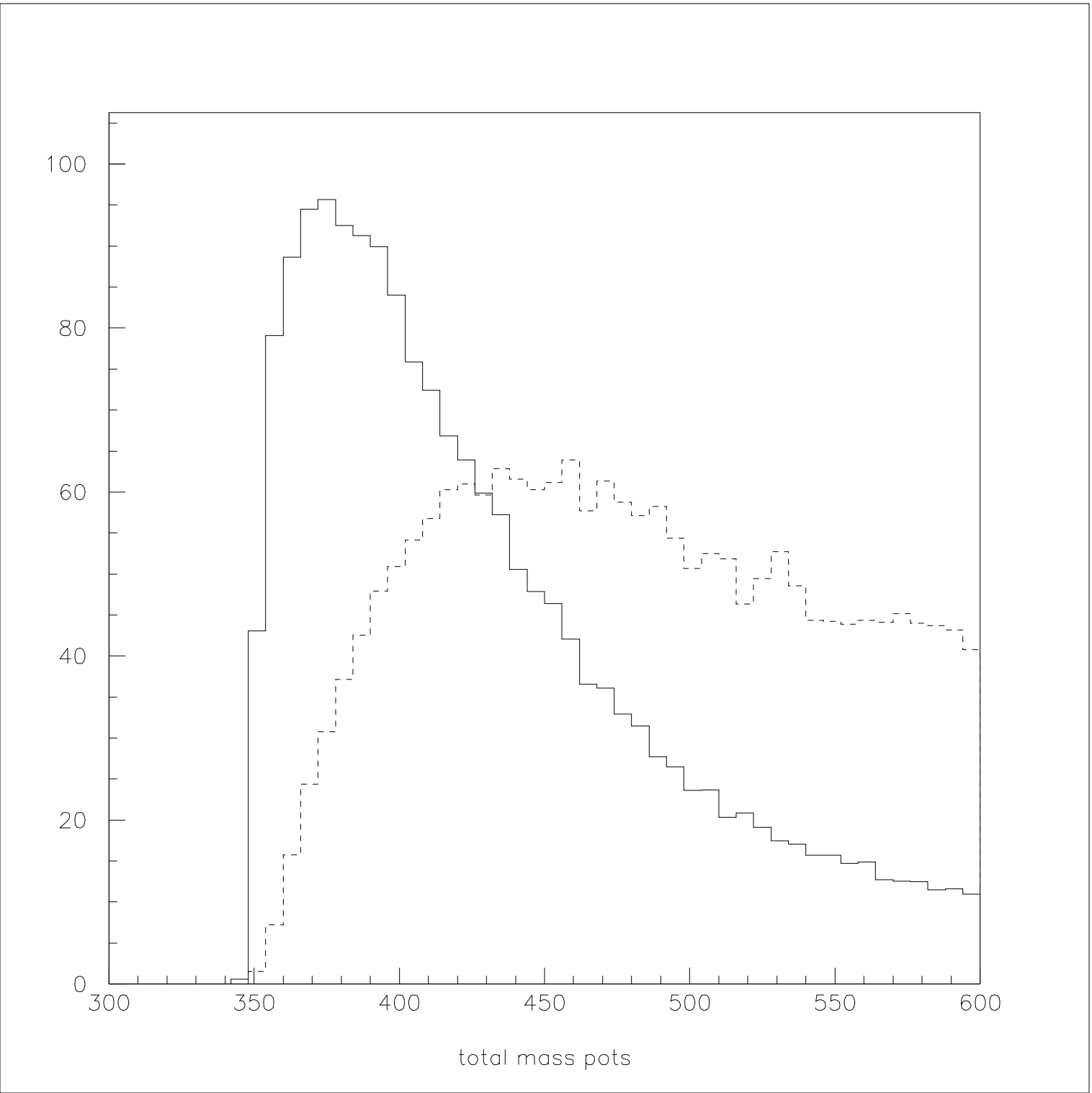
100
80
60
40
20
0
300
350
400
450
500
550
600
total mass pots